Обзор ArXiv: astro-ph, 12-16 июня 2017

От Сильченко О.К.

Astro-ph: 1706.03438

RECENTLY QUENCHED GALAXIES AT $z = 0.2 - 4.8$ IN THE COSMOS ULTRAVISTA FIELD

Akie Ichikawa[1,2] and Yoshiki Matsuoka[1,3]

ABSTRACT

We present a new analysis of the stellar mass function and morphology of recently-quenched galaxies (RQGs), whose star formation has been recently quenched for some reason. The COSMOS2015 catalog was exploited to select those galaxies at $0.2 < z < 4.8$, over 1.5 deg^2 of the Cosmic Evolution Survey (COSMOS) UltraVISTA field. This is the first time that RQGs are consistently selected and studied in such a wide range of redshift. We find increasing number density of RQGs with time in a broad mass range at $z > 1$, while low-mass RQGs start to grow very rapidly at $z < 1$. We also demonstrate that the migration of RQGs may largely drive the evolution of the stellar mass function of passive galaxies. Moreover, we find that the morphological type distribution of RQGs are intermediate between those of star-forming and passive galaxies. These results indicate that RQGs represent a major transitional phase of galaxy evolution, in which star-forming galaxies turn into passive galaxies, accompanied by the build up of spheroidal component.

Subject headings: galaxies: formation — galaxies: evolution — galaxies: high-redshift

Разбивка по цвету на пассивные, звездообразующие и с недавней остановкой звездообразования

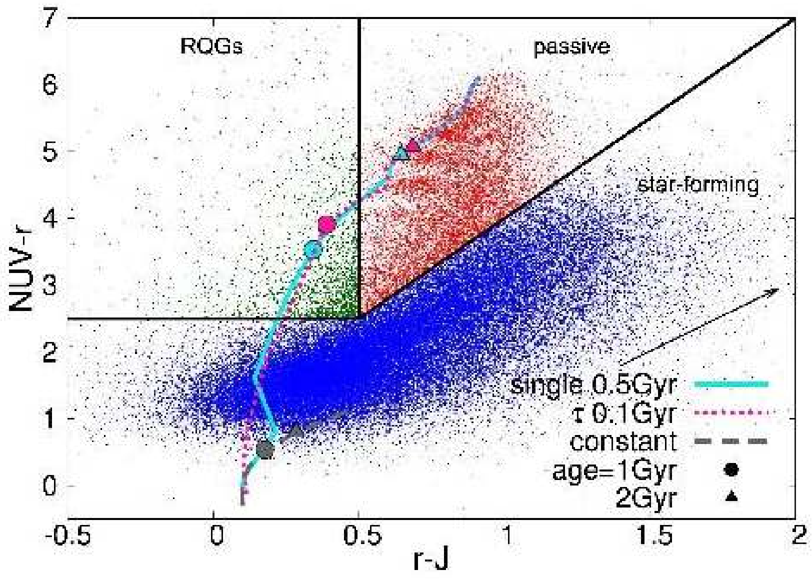

FIG. 1.— Rest-frame *NUV-r-J* color diagram. The blue, red and green dots represent star-forming galaxies, passive galaxies, and RQGs, respectively. The cyan, pink, and gray lines represent the color tracks of simple stellar populations by the single burst model, exponentially declining model, and constant star formation model, respectively (see text). The big dots and triangles mark the stellar ages of 1 and 2 Gyr, respectively, in each model. The arrow represents dust extinction corresponding to $A_V = 1$ mag (Calzetti et al. 2000).

Функции светимости

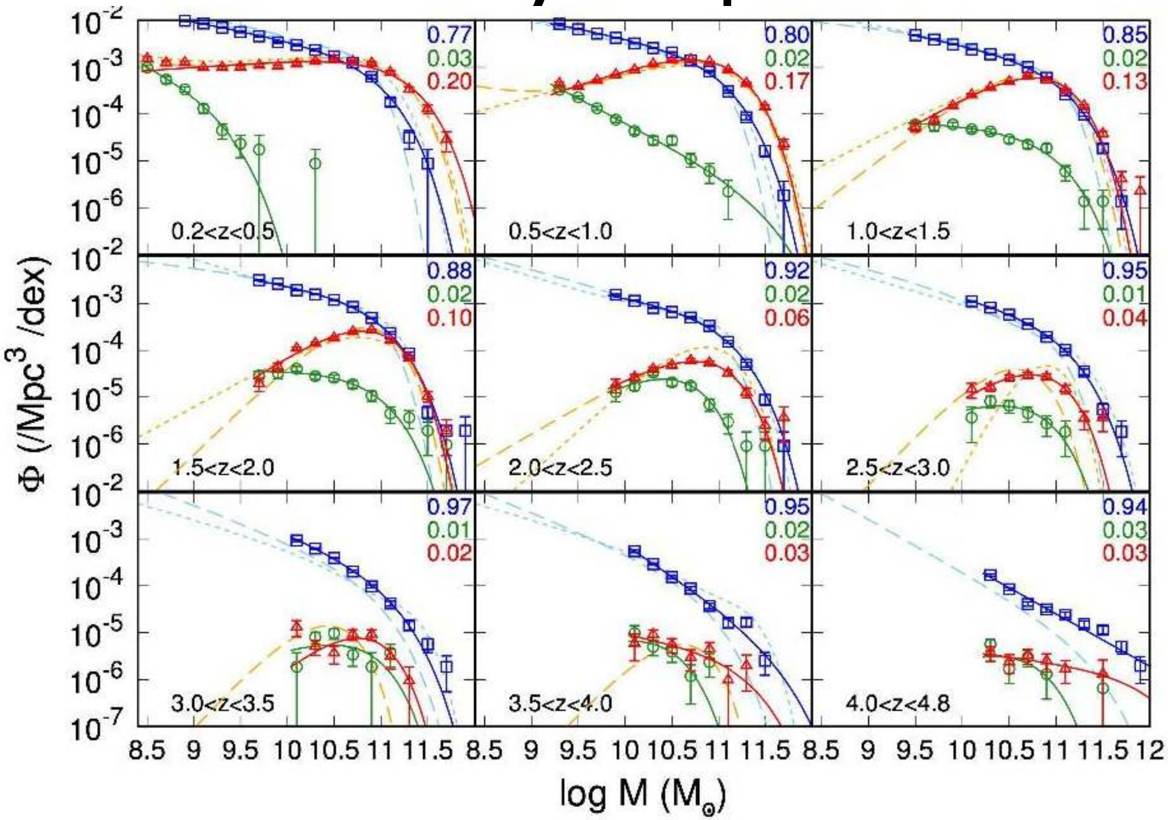

Сравнение функций светимости галактик разных типов в одну (каждую) эпоху

Эволюция функций светимости галактик разных типов

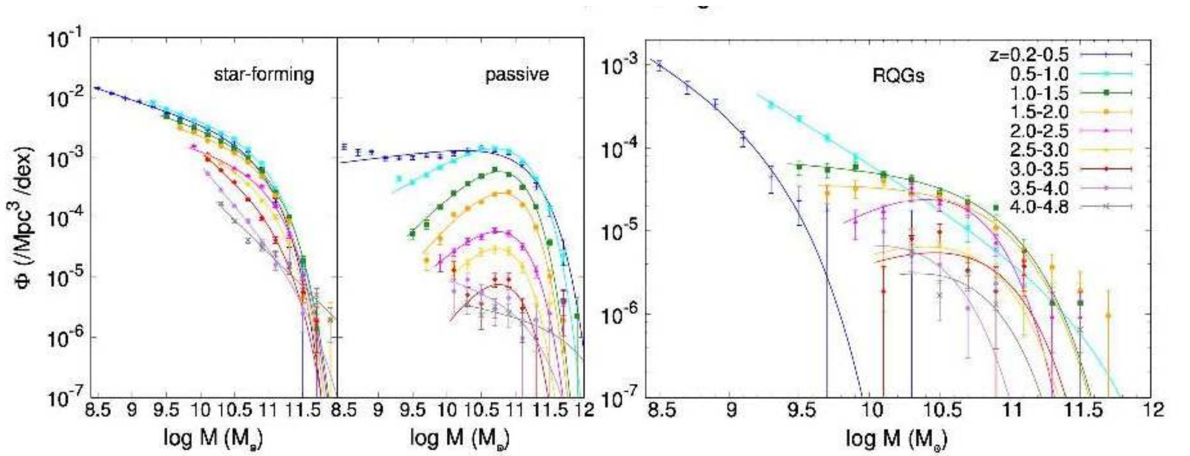

Модель: что, если галактики с остановкой SF через 0.5 (1) млрд лет становятся пассивными

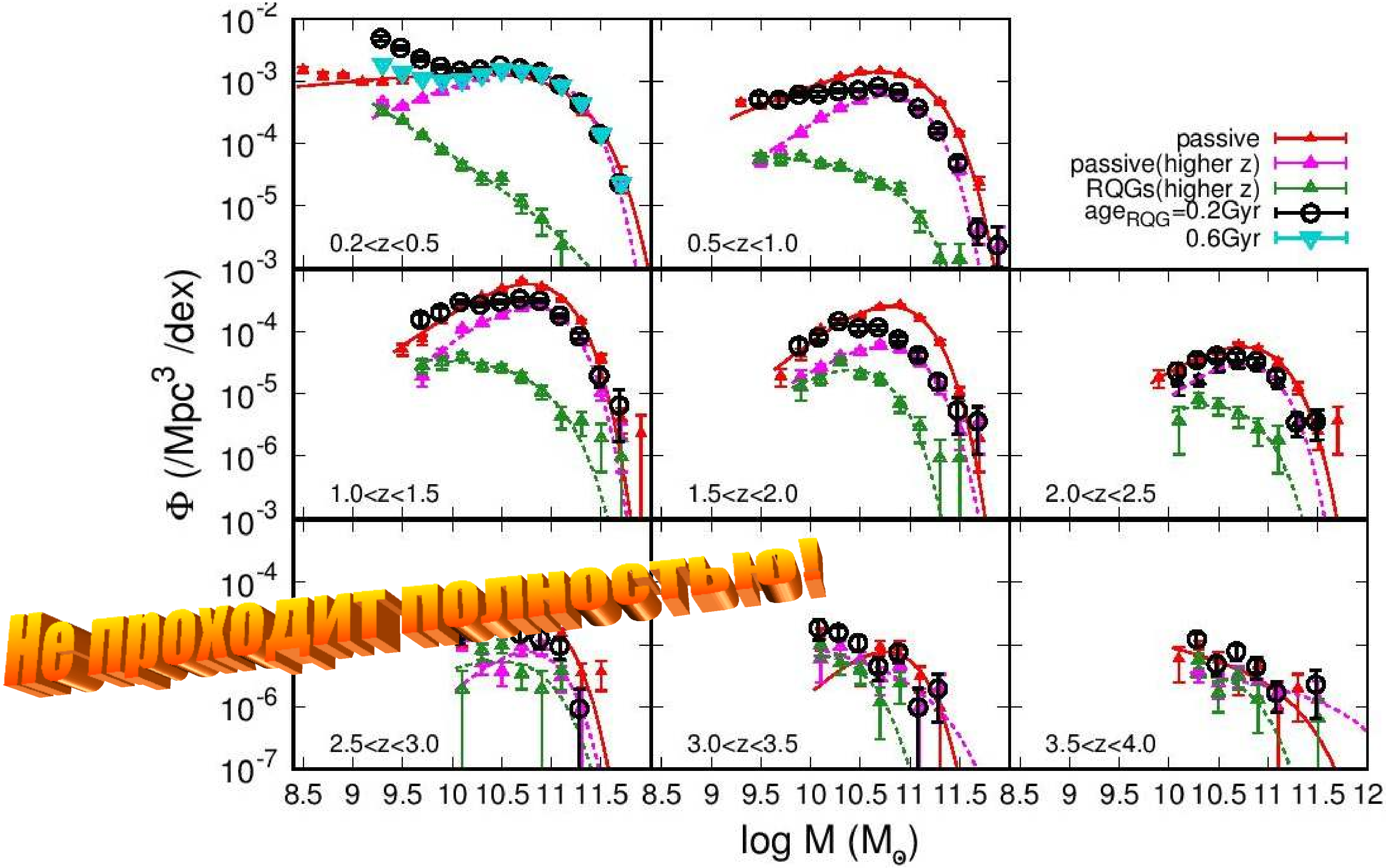

Распределение по морфологическим типам: в общем-то все ДИСКОВЫЕ

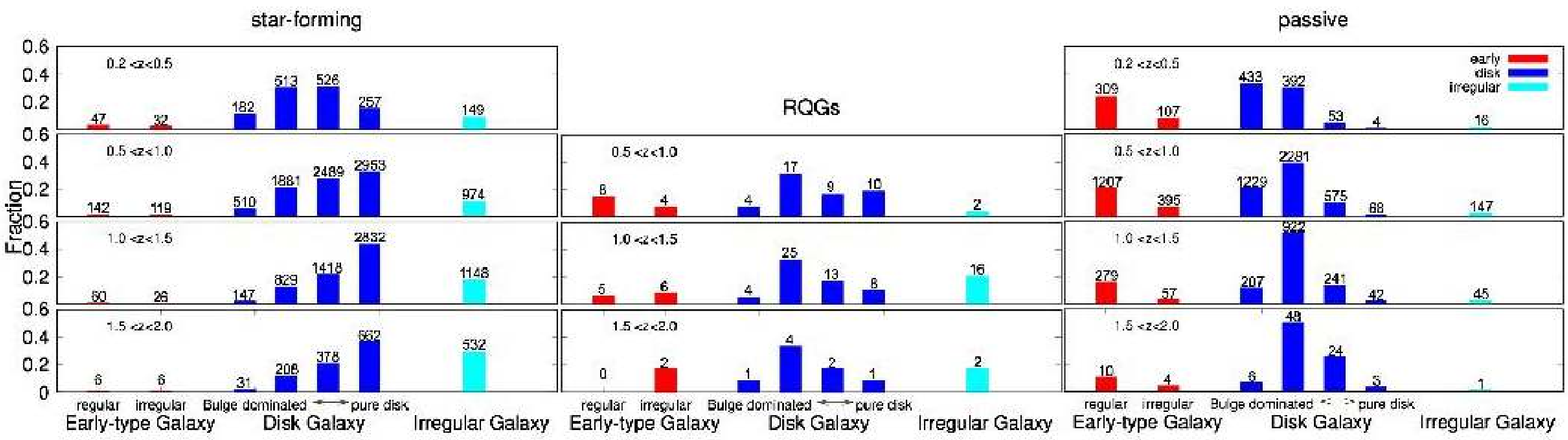

FIG. 4.— Fraction of each morphological type for the star-forming galaxies (left panel), RQGs (middle panel), and passive galaxies (right panel), based on the ZEST classification. The red, blue, and light-blue bars represent early, disk, and irregular-type galaxies, respectively, with subdivisions according to the irregularity and bulgeness (see text). The number of galaxies included in each morphological type is indicated above each bar.

Astro-ph: 1706.04248

HI KINEMATICS AND MASS DISTRIBUTION OF MESSIER 33

S. Z. Kam [1,2], C. Carignan[1,2,3], L. Chemin[4,5], T. Foster[6], E. Elson[3], T. H. Jarrett[3]

[1] Laboratoire de Physique et de Chimie de l'Environnement, Observatoire d'Astrophysique de l'Université Ouaga I Pr Joseph Ki-Zerbo (ODAUO), 03 BP 7021, Ouaga 03, Burkina Faso; **email: szachkam@gmail.com**

[2] Département de physique, Université de Montréal, C.P. 6128, Succ. centre-ville, Montréal, Québec, Canada, H3C 3J7

[3] Department of Astronomy, University of Cape Town, Private Bag X3, Rondebosch 7701, South Africa; **email: ccarignan@ast.uct.ac.za**

[4] INPE/MCT, Divisão de Astrofísica, Av. dos Astronautas, 1.758, São Jose dos Campos, SP, 12227-010, Brazil

[5] Universidad de Antofagasta, Unidad de Astronomía, Antofagasta, Avenida Angamos 601, Antofagasta 1270300, Chile; **email: laurent.chemin@uantof.cl**

[6] Dominion Radio Astrophysical Observatory, P.O. Box 248, Penticton, British Columbia, V2A 6J9, Canada

ABSTRACT

A new deep HI survey of the galaxy Messier 33 is presented, based on observations obtained at the Dominion Radio Astrophysical Observatory. We observe a perturbed outer gas distribution and kinematics in M33, and confirm the disk warping as a significant kinematical twist of the major axis of the velocity field, though no strong tilt is measured, in agreement with previous work. Evidence for a new low brightness HI component with anomalous velocity is reported. It harbours a large velocity scatter, as its kinematics both exceeds and lags the rotation of the disk, and leaks in the forbidden velocity zone of apparent counter-rotation. The observations also reveal wide and multiple peak HI profiles which can be partly explained by crowded orbits in the framework of the warp model. Asymmetric motions are identified in the velocity field, as possible signatures of a lopsided potential and the warp. The mass distribution modeling of the hybrid Hα-HI rotation curve favours a cuspy dark matter halo with a concentration in disagreement with the ΛCDM dark halo mass-concentration relationship.

Что такое М33:

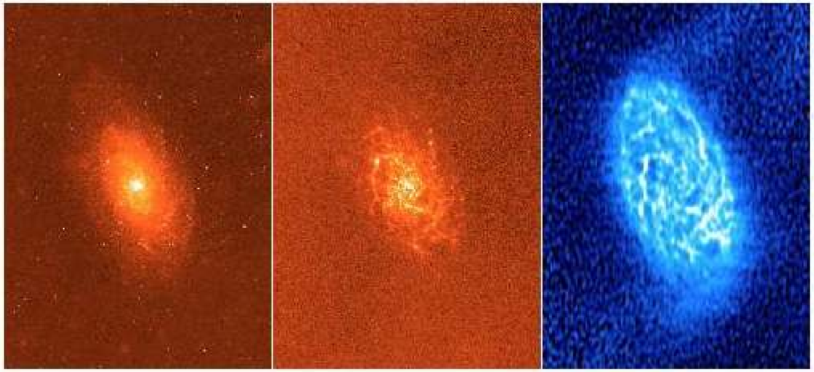

Figure 1. WISE W1 (left), W3 (center) and the inner bright HI disk (right) of M33.

Table 2. Summary of the six 21 cm HI line synthesis fields centred on and surrounding M33, carried out with the DRAO Synthesis Telescope.

Observ. Date	Field Centre (RA, DEC) (J2000.0)	Beam Parameters $\theta_{maj}(') \times \theta_{min}(')$, CCWE
09/29/08	$01^h33^m50.9^s$, $+30°39'36''$	$1.90 \times 0.97'$, $-89.69°$
09/29/08	$01^h36^m10.2^s$, $+31°50'34''$	1.85×0.97, $-89.82°$
11/05/08	$01^h31^m38.2^s$, $+29°28'12''$	1.98×0.97, $-89.91°$
11/05/08	$01^h34^m45.8^s$, $+31°08'13''$	1.86×0.97, $-90.11°$
12/04/08	$01^h32^m56.4^s$, $+30°11'01''$	1.94×0.97, $-90.30°$
12/04/08	$01^h33^m50.9^s$, $+30°39'36''$	$1'.91 \times 0'.97$, $-90.49°$

Table 1. Parameters of M 33.

Parameters	Value	Source
Morphological type	SA(s)cd	RC3
R.A. (2000)	$01^h\ 33^m\ 33.1^s$	RC3
Dec. (2000)	$+30°\ 39'\ 18''$	RC3
Systemic Velocity (km s^{-1})	-179 ± 3	RC3
Distance (Mpc)	0.84	
Scale (pc/arcmin)	244	
Disk Scale length (kpc)	1.6 (@ 3.6 μm)	Kam15
Optical radius, R_{25}	$35'.4 \pm 1'.0$	RC3
Inclination, i	$52° \pm 3°$	WWB
Position angle (major axis)	$22.5° \pm 1°$	WWB
Apparent magnitude, m_V	5.28	RC3
Absolute magnitude, M_V	-19.34	
Total HI mass ($M_\odot$)	$1.95\ 10^9$	Sec. 2
Systemic Velocity (km s^{-1})	-180 ± 3	Sec. 2
V_{rot} maximum (km s^{-1})	125	Sec. 4
Stellar mass ($M_\odot$), mass models	$5.5\ 10^9$	Sec. 5
Dynamical mass ($M_\odot$), inside $R = 23$ kpc	$7.9\ 10^{10}$	Sec. 5

RC3: de Vaucouleurs et al. (1991); Kam15: Kam et al. (2015); WWB: Warner et al. (1973). See Kam15 for the distance to M33, as based on a compilation of distance moduli from TRGB, Cepheids and Planetary Nebula Luminosity Function methods.

Чего только нет в PV-диаграммах HI: противовращение, warp…

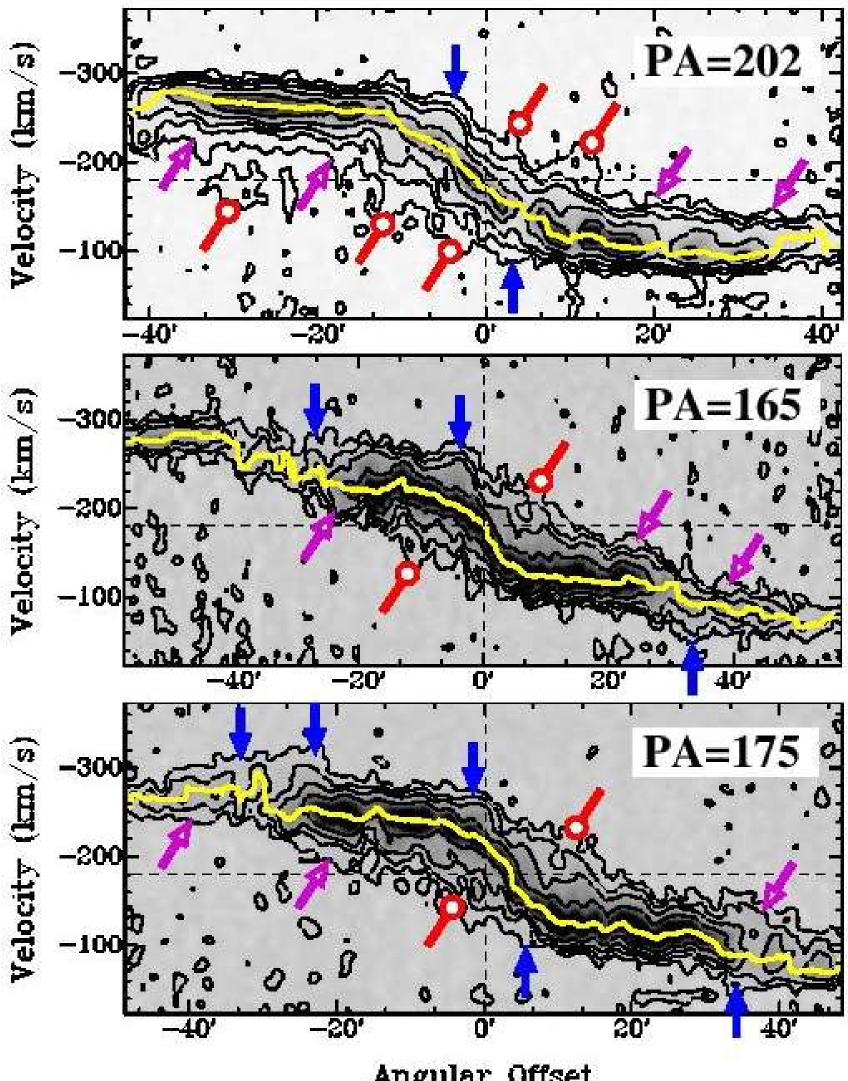

Результирующие карты

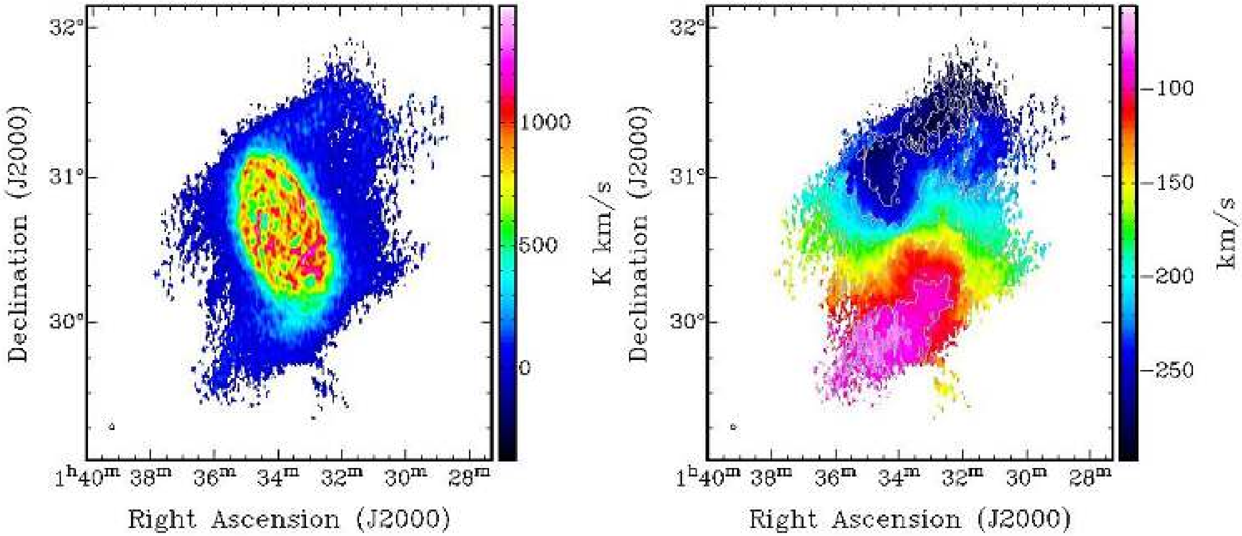

Figure 6. HI integrated emission map and velocity field of Messier 33 (left and right panels, respectively). The velocity contours are −280, −260, −220, −180, −140, −100, and −80 km s^{-1}. The circle to the bottom left of each panel represents the 2′ resolution.

Дисперсия скоростей HI

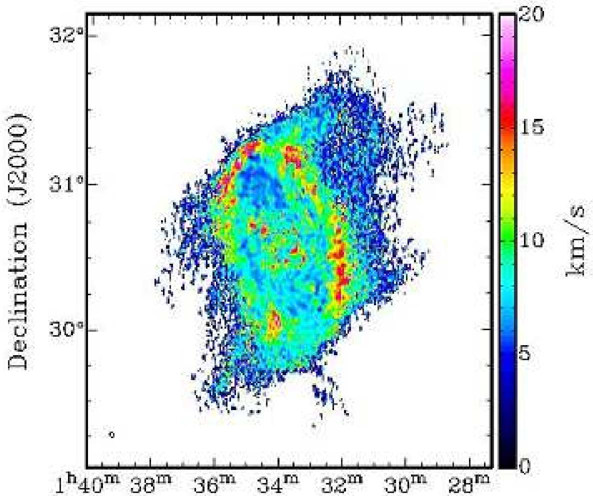

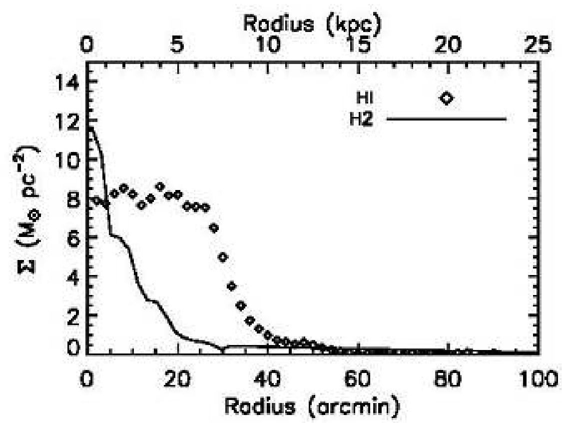

Figure 8. HI mass surface density profile of M33 (symbols). The molecular gas mass surface density (solid line) is from Druard et al. (2014).

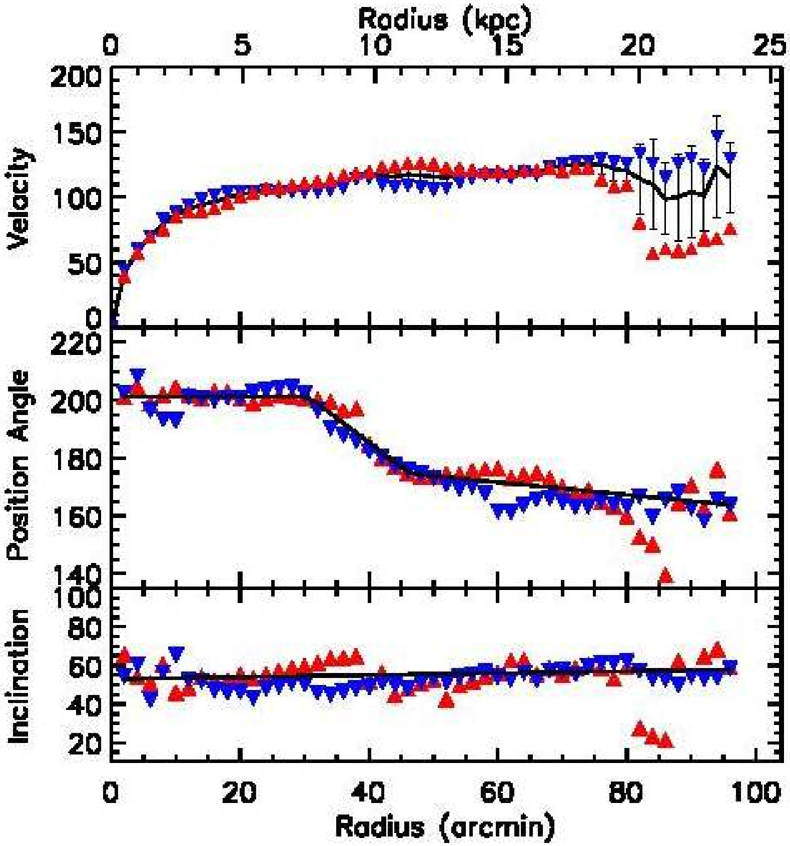

Figure 9. Results of the tilted-ring model of the HI velocity field of M33. The top panel shows the rotation curve (in km s^{-1}), the middle panel the major axis position angle (in °) and the bottom panel the inclination (in °). Red downward triangles are the results for the receding side, blue upward triangles those for the approaching side.

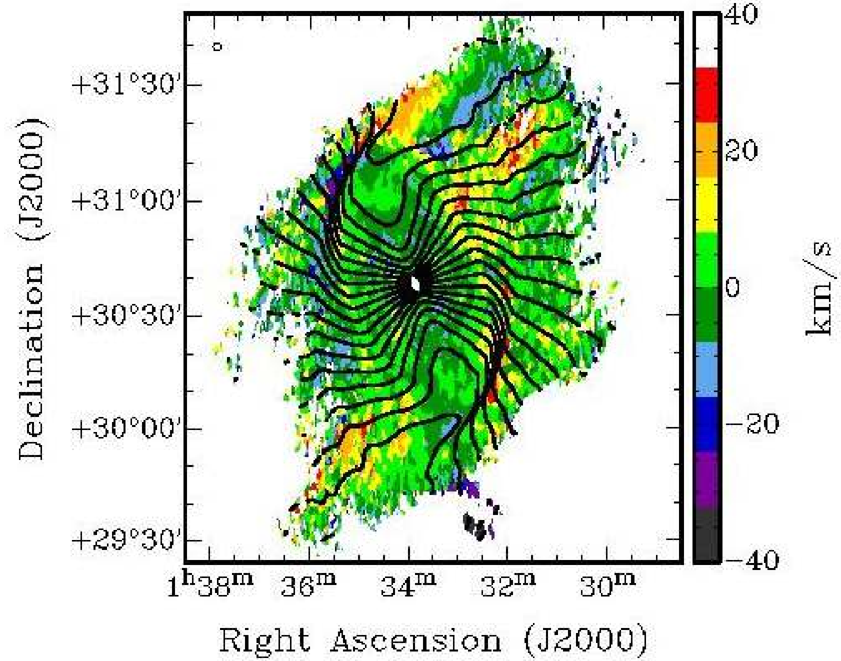

Figure 12. M33 residual velocity field (observation minus model). The model velocity field is represented by the contours, from -90 to -280 km s^{-1} by step of 10 km s^{-1}. The circle to the upper left corner represents the 2′ resolution.

Остаточные скорости после вычитания tilted-ring модели

Анализ двумерного поля скоростей методом наклонных колец

Динамические модели

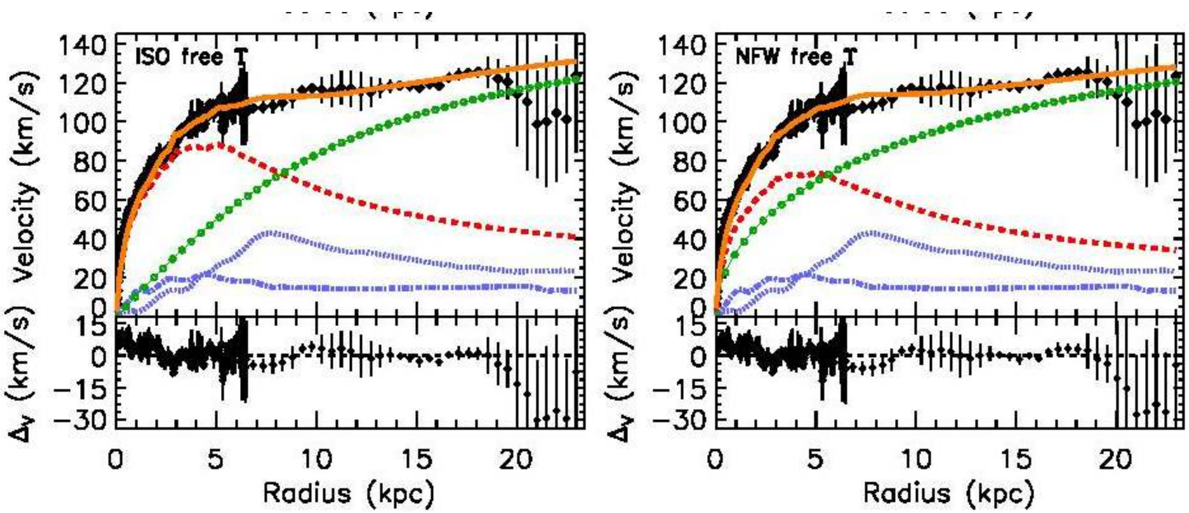

Dark matter

Figure 15. Mass distribution models of M33 with the ISO (left column) and NFW (right column) haloes. From top to bottom, results are shown for different values of the stellar disk mass-to-light ratio: fixed Υ = 0.52, fixed Υ = 0.72 and free, best-fit Υ, where the fixed values were inferred from stellar population models (see text). Black filled symbols represent the observed data, a solid orange line the model of the total velocity curve, a dashed red line the contribution from the stellar disk, dotted and dashed-dotted blue lines those from the atomic and molecular gas disks, respectively, and a circle green line that from the dark matter halo. For each sub-panel, the bottom insert shows the velocity residual velocity curve Δ_V (observed minus modeled rotation curves).

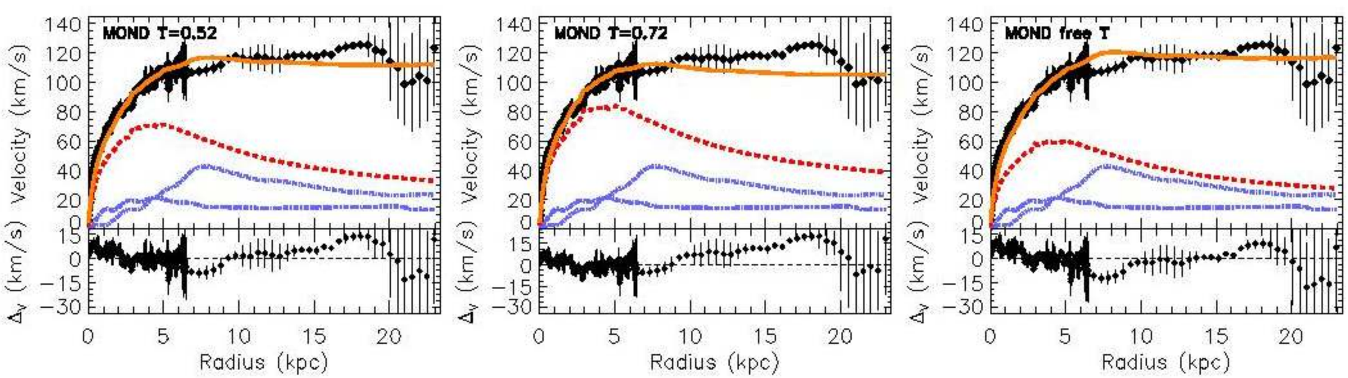

MOND

Figure 16. Mass distribution models of M33 with MOND (standard interpolation function). Symbols and lines are the same as in Fig. 15.

Astro-ph: 1706.04754

The SAMI Galaxy Survey: energy sources of the turbulent velocity dispersion in spatially-resolved local star-forming galaxies

Luwenjia Zhou[1,2,3*], Christoph Federrath[2], Tiantian Yuan[2], Fuyan Bian[2,7], Anne M. Medling[2,4,5], Yong Shi[2,3], Joss Bland-Hawthorn[8], Julia J. Bryant[6,8,10], S. Brough[13], Barbara Catinella[14], Scott M. Croom[8,10], Michael Goodwin[6], Gregory Goldstein[11], Andrew W. Green[6], Iraklis S. Konstantopoulos[6,12], J.S. Lawrence[6], Matt S. Owers[6,11], Samuel N. Richards[8,9,10], S. F. Sanchez[15]

[1] *School of Astronomy and Space Science, Nanjing University, Nanjing 210093, China*
[2] *Research School of Astronomy & Astrophysics, Australian National University, Canberra, ACT 2611, Australia*
[3] *Key Laboratory of Modern Astronomy and Astrophysics (Nanjing University), Ministry of Education, Nanjing 210093, China*
[4] *Cahill centre for Astronomy and Astrophysics, California Institute of Technology, MS 249-17, Pasadena, CA 91125, USA*
[5] *Hubble Fellow*
[6] *Australian Astronomical Observatory, PO Box 915, North Ryde NSW 1670, Australia*
[7] *Stromlo Fellow*
[8] *Sydney Institute for Astronomy (SIfA), School of Physics, The University of Sydney, NSW 2006, Australia*
[9] *Australian Astronomical Observatory, 105 Delhi Rd, North Ryde, NSW 2113, Australia*
[10] *ARC Centre of Excellence for All-sky Astrophysics (CAASTRO)*
[11] *Department of Physics and Astronomy, Macquarie University, NSW 2109, Australia*
[12] *Atlassian 341 George St Sydney, NSW 2000*
[13] *School of Physics University of New South Wales NSW 2052 Australia*
[14] *ICRAR, M468, The University of Western Australia, 35 Stirling Highway, Crawley, WA 6009, Australia*
[15] *Instituto de Astronomía, Universidad Nacional Autonóma de México, A.P. 70-264, 04510 México, D.F., Mexico*

Парметры наблюдений, пример результатов

Table 1. Red and blue data cubes from LZIFU.

data cube	$\lambda^{\dagger}$	R‡	σ^{*}
Blue	3700 – 5700	1730	74 km s^{-1}
Red	6250 – 7350	4500	29 km s^{-1}

† Wavelength range.
‡ Spectral resolution. Full width half (FWHM) = c/R.
* Velocity resolution according to spect tion.

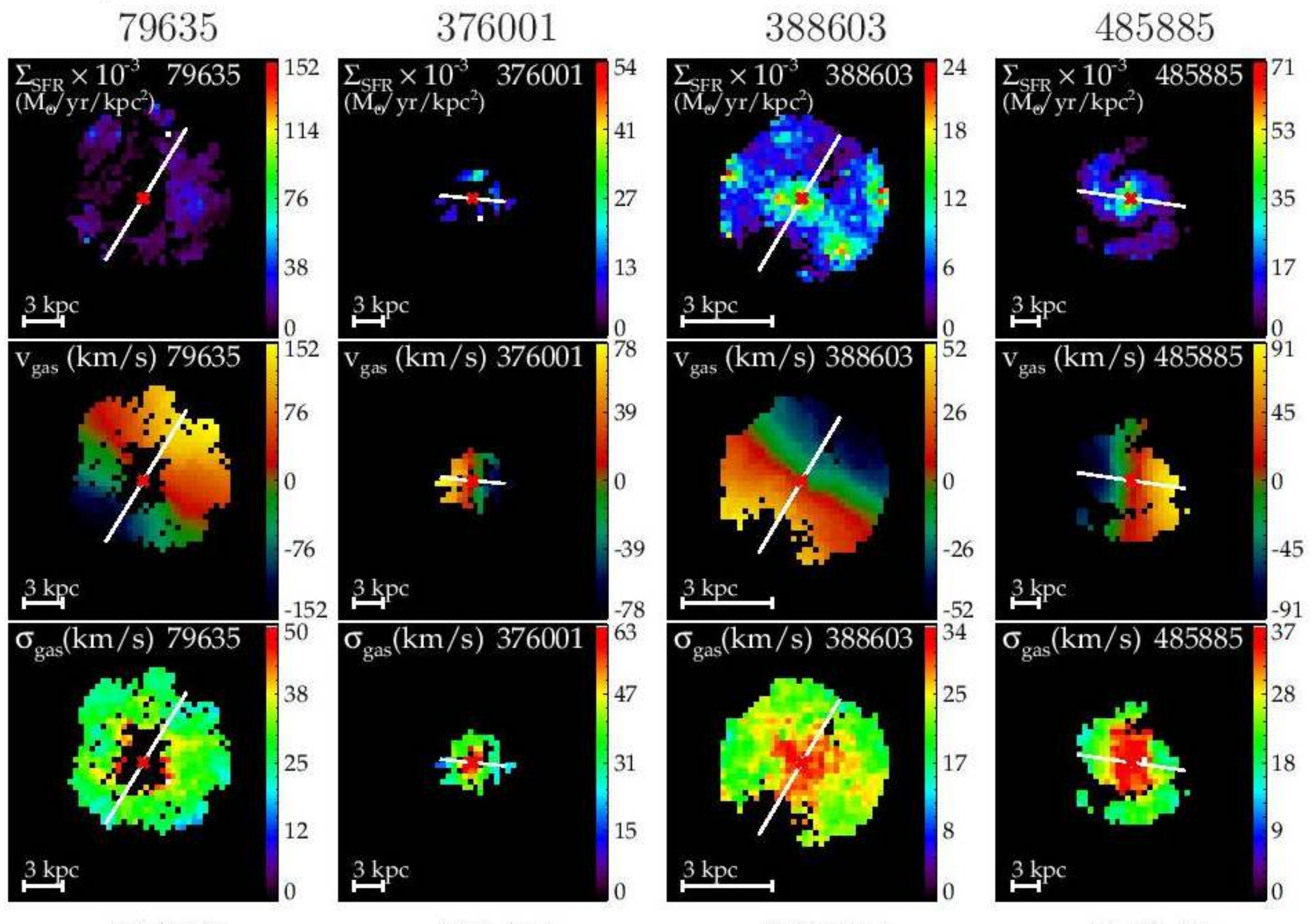

Выборка

Table 2. Properties of the eight star-forming galaxies in our final sample of star-forming SAMI galaxies.

CATID	RA [hh: mm: ss]	DEC [dd: mm: ss]	redshift	stellar mass[1] $[M_\odot]$	radius[2] [″]	[kpc]	ellip[3]	i [4] [°]	σ_{gas} [5] [km s^{-1}]	Σ_{SFR} [6] $[M_\odot\ yr^{-1}\ kpc^{-2}]$
79635	14 50 03.3	43 51 03.1	0.040	2.9×10^{10}	9.13	7.8	0.40	55.0	28 ± 4	0.019 ± 0.009
376001	08 46 31.3	00 05 51.0	0.051	1.8×10^{10}	2.41	2.7	0.07	22.4	31 ± 9	0.022 ± 0.007
388603	09 23 08.1	02 29 09.9	0.017	6.3×10^{9}	14.3	5.2	0.12	28.6	24 ± 4	0.009 ± 0.003
485885	14 31 01.9	-01 43 02.0	0.055	1.8×10^{10}	5.04	6.0	0.16	33.6	24 ± 4	0.014 ± 0.005
504882	14 30 15.3	-01 55 56.2	0.054	1.3×10^{10}	3.80	4.4	0.19	37.0	20 ± 2	0.010 ± 0.003
508421	14 27 57.4	-01 37 52.3	0.055	2.5×10^{10}	3.74	4.5	0.26	43.0	87 ± 44	0.076 ± 0.016
599582	08 48 45.6	00 17 29.5	0.053	6.2×10^{10}	9.60	11	0.32	48.6	26 ± 5	0.020 ± 0.009
618152	14 18 05.5	00 13 38.6	0.053	1.0×10^{10}	3.56	4.1	0.29	46.1	24 ± 3	0.023 ± 0.010

[1] Stellar masses are from the GAMA survey (Taylor et al. 2011).
[2] Effective radius, i.e., half light radius, also from the GAMA survey (Kelvin et al. 2012).
[3] Ellipticity is from the GAMA survey (http://www.gama-survey.org/dr2/tools/sov.php). We use the GAL_ELLIP_R to get the R-band axis ratio. The relation between minor-to-major axis ratio and ellipticity is: $b/a = 1$ - ellipticity.
[4] Inclination angle. The calculation is based on classical Hubble formula: $\cos^2 i = ((b/a)^2 - q_0^2)/(1 - q_0^2))^{1/2}$, where b/a is the minor-to-major axis ratio, i is the inclination angle and $q_0 = 0.2$ ($i = 90°$ for $b/a < q_0$).
[5] Flux weighted global gas velocity dispersion. Only the pixels with $\sigma_{gas} > 2\ v_{grad}$ are considered (see more in Section 2.2.3).
[6] Flux weighted SFR surface density. Only the pixels with $\sigma_{gas} > 2\ v_{grad}$ are considered (see more in Section 2.2.3).

По-пиксельная турбулентность (ширина эмиссионных линий)

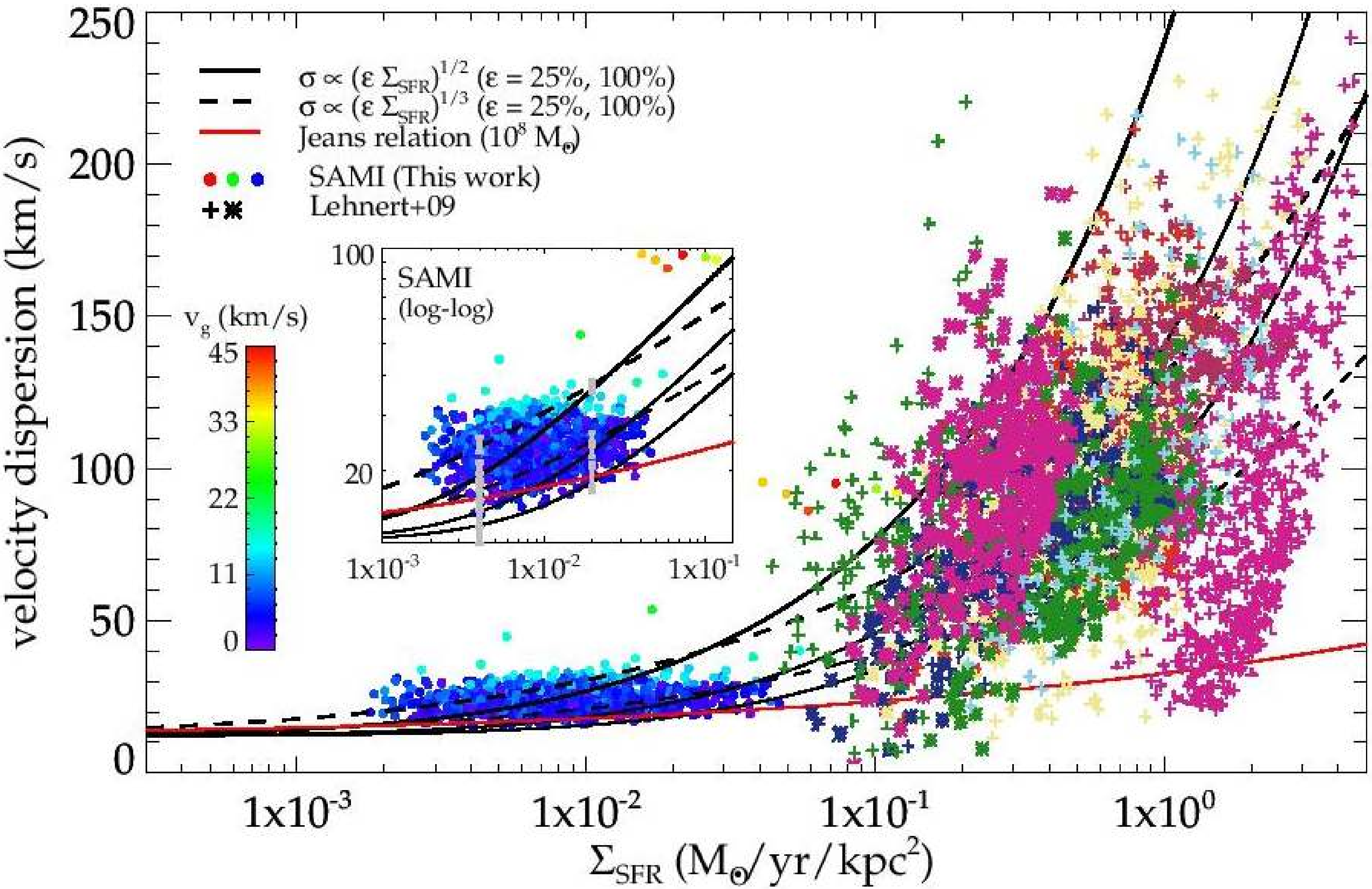

То же самое, осредненное в масштабах всей галактики

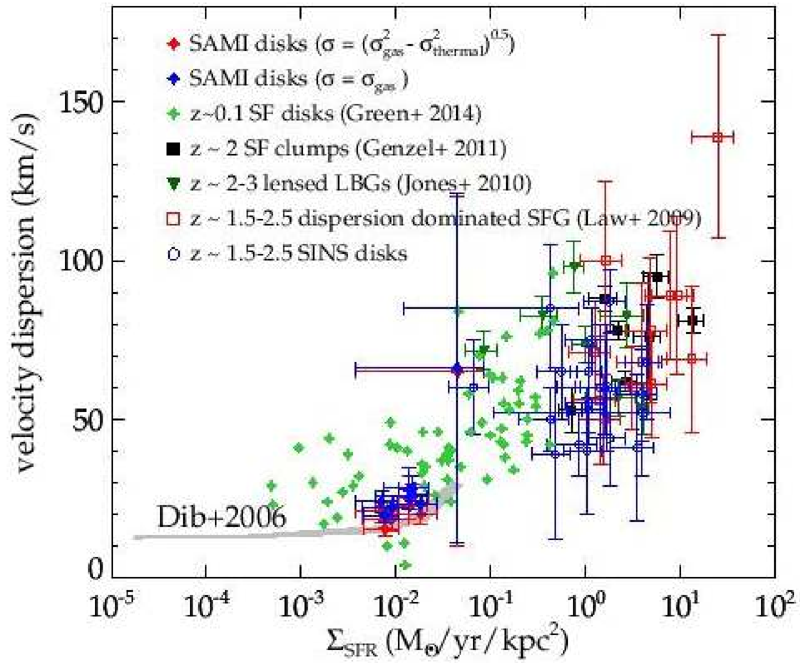

Figure 4. Global dependence of σ_{gas} on Σ_{SFR}. Our eight SAMI galaxies compared to local high Hα luminosity galaxies from Green et al. (2014) and $z > 1$ star-forming galaxies and clumps (see Section 3.2.2 for further details). Each blue (red) filled diamond shows one entire galaxy in our sample including (excluding) the contribution from thermal broadening ($\sigma_{thermal} \sim 12$ km s^{-1}, Glazebrook 2013). For the measurement of σ_{gas} and Σ_{SFR}, see footnotes in Table 2. Green diamonds refer to the Hα luminous galaxies in Green et al. (2014). The black filled squares, dark green triangles, red open squares and blue open circles refer to the $z > 1$ star-forming galaxies and clumps. The grey con-